

**NANO EXPRESS**

**Open Access**

# Room-temperature nonequilibrium growth of controllable ZnO nanorod arrays

Qian Li, Kui Cheng, Wenjian Weng\*, Chenlu Song, Piyi Du, Ge Shen and Gaorong Han

## Abstract

In this study, controllable ZnO nanorod arrays were successfully synthesized on Si substrate at room temperature (approx. 25°C). The formation of controllable ZnO nanorod arrays has been investigated using growth media with different concentrations and molar ratios of  $\text{Zn}(\text{NO}_3)_2$  to NaOH. Under such a nonequilibrium growth condition, the density and dimension of ZnO nanorod arrays were successfully adjusted through controlling the supersaturation degree, i.e., volume of growth medium. It was found that the wettability and electrowetting behaviors of ZnO nanorod arrays could be tuned through variations of nanorods density and length. Moreover, its field emission property was also optimized by changing the nanorods density and dimension.

## Introduction

One-dimensional (1D) nanostructures, such as nanorods, nanowires, and nanotubes, have extensively been investigated in recent years for their excellent optoelectronic, electronic, mechanical, magnetic, photochemical properties, etc. [1-6]. The density, morphology, crystal size, and dimension of 1D nanostructure arrays are very important as they strongly determine the properties of the arrays, such as wettability, field emission property, photochemical property, etc. [7-9]. Müller et al. [10] have found that the contact angle increased as the density of Ge nanopramids grown on Si substrate increased. Lau et al. [11] studied the wettability of poly-coated carbon nanotube array and demonstrated the contact angle increased when the height of nanotube increased. Among various nanomaterials, zinc oxide (ZnO) nanostructure has attracted much attention mainly because of its wide direct band gap (3.37 eV), large excitation binding energy (60 meV), optical transparency, electric conductivity, piezoelectricity, and so on [12]. Especially, many studies have been carried out on 1D ZnO nanorod because of its novel physical properties and potential applications in various nanostructure devices [13-19]. Numerous techniques to fabricate ZnO nanorod arrays on substrates have been reported, including metal-organic chemical vapor deposition [16], vapor transport process [17], solution chemical route [18-21], molecular

beam epitaxy [22], pulsed laser deposition [23], electrochemical deposition [24], and thermal evaporation [25]. Among them, room temperature solution route is particularly attractive because of its low cost, facile synthesis, high efficiency, and various substrates choices. Several techniques have been reported for growing ZnO nanorods at room temperature. Electrochemical deposition technique is one among them [26], but this method is restricted to electrode area or the substrate property. In addition, wet chemical route to fabricate dense ZnO nanorods array on Zn foil [27] at room temperature has been reported, which is not applicable to various substrates.

The properties of ZnO nanorods are greatly influenced by the density, morphology and dimension of the arrays [28-31]. Therefore, room temperature preparation of ZnO nanorods arrays synthesized on different substrates with controllable morphologies and densities is quite required as it could favor and speed up the applications of 1D ZnO nanostructures. Meanwhile, the specialty of room temperature solution method is that the whole formation processes of ZnO nanostructures are out of equilibrium. The dynamic variations of supersaturation degree strongly influence the process of nonequilibrium growth in the solution. Although nanostructures could be synthesized by this nonequilibrium growth method, the nanostructure arrays with controlled morphology, density, and dimension are difficult to achieve.

In this study, the room temperature (approx. 25°C) solution growth of density- and dimension-controlled ZnO nanorod arrays in a nonequilibrium condition was

\* Correspondence: wengwj@zju.edu.cn  
Department of Materials Science & Engineering, State Key Laboratory of Silicon Materials, Zhejiang University, Hangzhou 310027, People's Republic of China

studied. The formation of ZnO nanorod arrays was influenced by the concentration of growth medium and the molar ratio of  $\text{Zn}(\text{NO}_3)_2$  to NaOH. The ZnO nanorod arrays with variable densities and dimensions were induced by tuning the volume of the growth medium, which resulted in a dynamic variations process of supersaturation degree. The wettability, electrowetting, and field emission properties of the ZnO nanorod arrays with different density and dimension were measured and discussed.

## Experimental

Clean Si (100) wafers ( $10 \times 10 \text{ mm}^2$ ) were used as substrates. For the preparation of ZnO seed-layer, 0.1-M zinc acetate dihydrate with ethanolamine in equimolar of  $\text{Zn}^{2+}$  was dissolved into 10-mL ethanol solution and stirred continuously for 20 min to be precursor solution. 15- $\mu\text{L}$  precursor solution aforesaid was spin-coated onto a clean Si substrate at 6000 rpm for 30 s. A seed-layer based on a Si substrate was formed after calcination at  $500^\circ\text{C}$  for 60 min. Then, an alkali growth medium containing  $\text{Zn}(\text{NO}_3)_2$  and NaOH aqueous solution for growing ZnO nanorods was prepared following  $\text{Zn}(\text{NO}_3)_2$  concentrations and molar ratios ( $R$ ) of  $\text{Zn}(\text{NO}_3)_2$  to NaOH tabulated in Table 1. Si substrates with seed-layers were vertically dipped in different volumes of growth medium solutions. After reaction at room temperature (approx.  $25^\circ\text{C}$ ) for 2 h, the substrates were rinsed with ethanol and deionized water thoroughly, final products were obtained after drying in air, as shown in Table 1 (samples A-E<sub>3</sub>).

Morphologies of the ZnO nanorods were observed in a field emission scanning electron microscope (Hitachi, S-4800). Phase and crystallinity of the nanorods were collected with an X-ray diffractometer (XRD, PANalytical, X'Pert PRO). The detailed structures of ZnO nanorods were investigated with a transmission electron microscope (TEM, JEOL, JEM-2010). The concentration of  $\text{Zn}^{2+}$  was determined by atomic absorption spectroscopy (AAS, Hitachi, 180-80). The wettability and electrowetting behaviors were measured by water contact angle measurement

(OCA 20, DATAPHYSICS) at room temperature. The electrowetting process relied on the modification of contact angle by the application of a voltage in the 0-60 V range between the doped Si substrate and the 3- $\mu\text{L}$  droplet of deionized water. A thin Cu wire was used to achieve electrical contact with the droplet. The measurements of field emission were performed in a vacuum chamber with a pressure of about  $2 \times 10^{-4}$  Pa at room temperature and the ZnO nanorods prepared on Si substrates were used as the cathode. The distance between the cathode and the anode was 600  $\mu\text{m}$  and the measured field emission area was  $0.48 \text{ cm}^2$ .

## Results and discussions

### Controlled growth of ZnO nanorod arrays

There were several parameters affecting the growth characteristics of ZnO nanorod arrays, such as molar ratio of  $\text{Zn}^{2+}$  to  $\text{OH}^-$ , zinc ion concentration, and volume of the growth medium (absolute quantity of zinc ion). Figure 1 shows the SEM pictures of samples D<sub>1</sub>, D<sub>2</sub>, C, and D<sub>3</sub>, which reveal the effects of different  $R$  ratios on nanorods morphology. When  $R$  was high (1:4 and 1:6), nanosheets formed (Figure 1a,b). It is noteworthy that small tips appear on the edge of nanosheets when  $R$  is 1:6. It is considered that these tips show the transformation of nanostructure from nanosheet to nanorod. When  $R$  decreased to 1:8, uniform ZnO nanorods with sharp tips formed (Figure 1c). Further decreasing  $R$  to 1:10 led to the formation of wider nanorods (Figure 1d).

Influences of  $\text{Zn}(\text{NO}_3)_2$  concentrations on the final morphology of nanostructures when the value of  $R$  was fixed to 1:8 were also investigated, as shown in Figure 2. When the  $\text{Zn}(\text{NO}_3)_2$  concentration was lower than 0.05 M (samples E<sub>1</sub>, E<sub>2</sub>), few or nearly no nanorods formed (Figure 2a,b). Figure 2c shows that the wide and aggregated nanorods appeared if  $\text{Zn}(\text{NO}_3)_2$  concentration was 0.1 M (sample E<sub>3</sub>). The well-aligned nanorod array with sharp tips could only be acquired when the  $\text{Zn}(\text{NO}_3)_2$  concentration reached 0.25 M (Figure 2d).

In a strong alkaline aqueous medium,  $\text{Zn}^{2+}$  ions are known to react readily with  $\text{OH}^-$  ions to form  $\text{Zn}(\text{OH})_4^{2-}$

**Table 1 Preparation conditions for different samples**

Zinc concentration (M)	$R$ (molar ratio of $\text{Zn}^{2+}/\text{OH}^-$ )	Medium volume (mL)	Sample Name
0.25	1:8	2	A
0.25	1:8	10	B
0.25	1:8	20	C
0.25	1:4	20	D <sub>1</sub>
0.25	1:6	20	D <sub>2</sub>
0.25	1:10	20	D <sub>3</sub>
0.025	1:8	20	E <sub>1</sub>
0.05	1:8	20	E <sub>2</sub>
0.1	1:8	20	E <sub>3</sub>

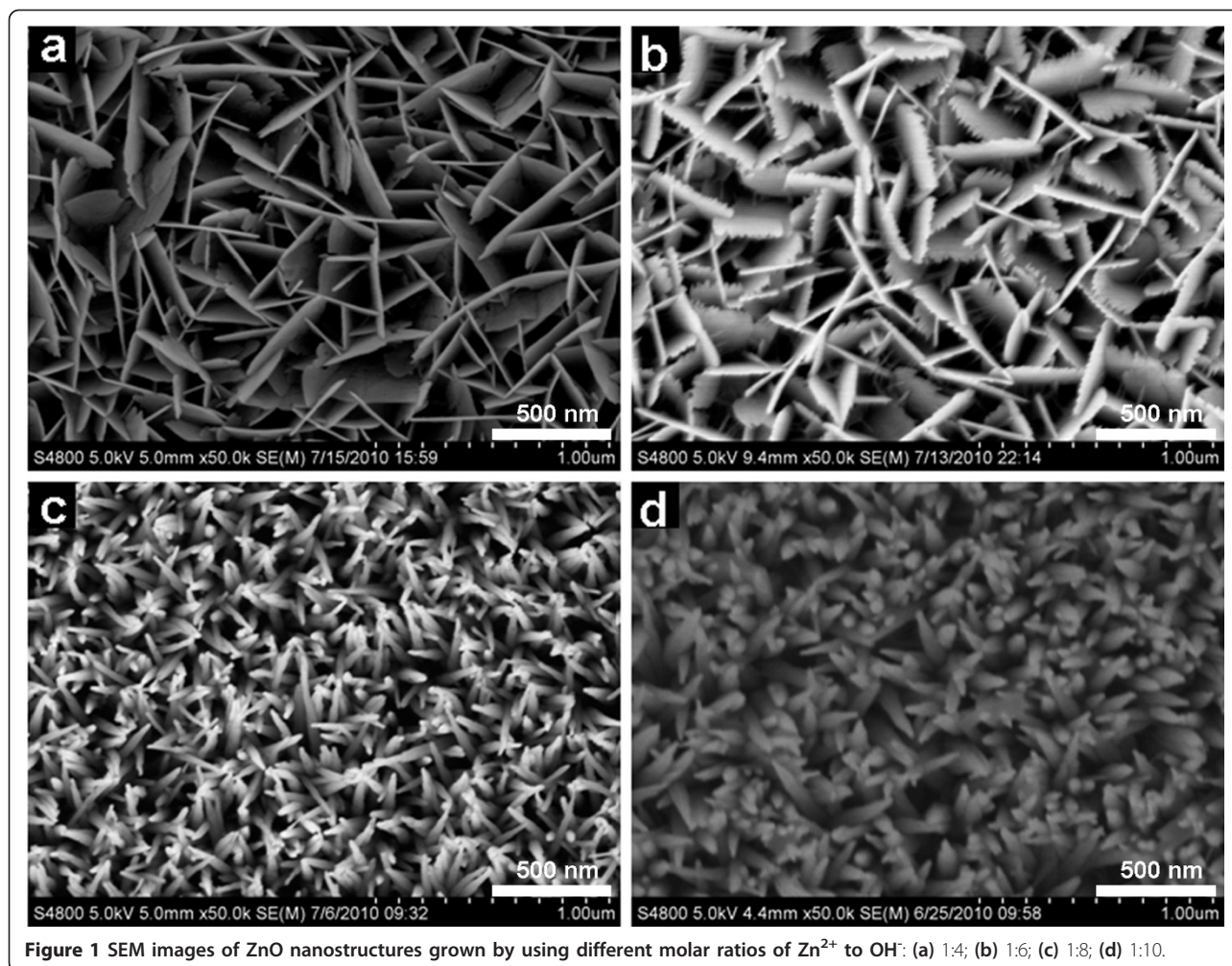
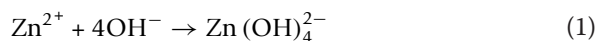


**Figure 1** SEM images of ZnO nanostructures grown by using different molar ratios of Zn<sup>2+</sup> to OH<sup>-</sup>: (a) 1:4; (b) 1:6; (c) 1:8; (d) 1:10.

complex species which act as the growth units for growing ZnO nanostructures along *c*-axis. Therefore, the main chemical reactions in alkaline zincate solution can simply be represented by the following equations:



Since the existence of ZnO seed-layer can reduce the nucleation energy barrier and the lattice mismatch effectively, pre-coating the substrate with seeds of ZnO provides proper conditions for heterogeneous nucleation and crystal growth.

The final morphologies of the nanostructures are determined by several factors during the growth process. The two most important factors are the concentration of Zn<sup>2+</sup> ions and OH<sup>-</sup> ions. The supersaturation of nonequilibrium growth medium is the key driving force for ZnO nanorods formation. On the one hand, supersaturated OH<sup>-</sup> in the medium induces sufficient Zn(OH)<sub>4</sub><sup>2-</sup> for

ZnO crystal growth. Higher Zn(OH)<sub>4</sub><sup>2-</sup> concentration will accelerate the reactions to form ZnO. On the other hand, the growth rate along *c*-axis direction can be reduced because superfluous OH<sup>-</sup> ions are easily adsorbed on the positively charged (0001)-Zn polar surface [32] and eventually lead to the formation of nanosheets (Figure 1a,b). However, for a fix Zn(NO<sub>3</sub>)<sub>2</sub> concentration, the amount of OH<sup>-</sup> ions can only be tuned over a small range for producing well-aligned nanorod arrays, in which the shielding effect of OH<sup>-</sup> ions seems to be weakened compared with the acceleration of the growth rate along the *c*-axis direction. When *R* is too high, zinc hydroxide species form precipitation from the solution; if *R* is too low, the seed-layer would be etched away. Moreover, certain Zn(NO<sub>3</sub>)<sub>2</sub> concentration is the guarantee of a supersaturated medium for the crystallization because ZnO nanorods cannot grow well with the low concentration of Zn(OH)<sub>4</sub><sup>2-</sup> [33].

Under the best condition for the growth of ZnO nanorod, density, and length, controlled growth of ZnO nanorods was investigated. The commonest ways to



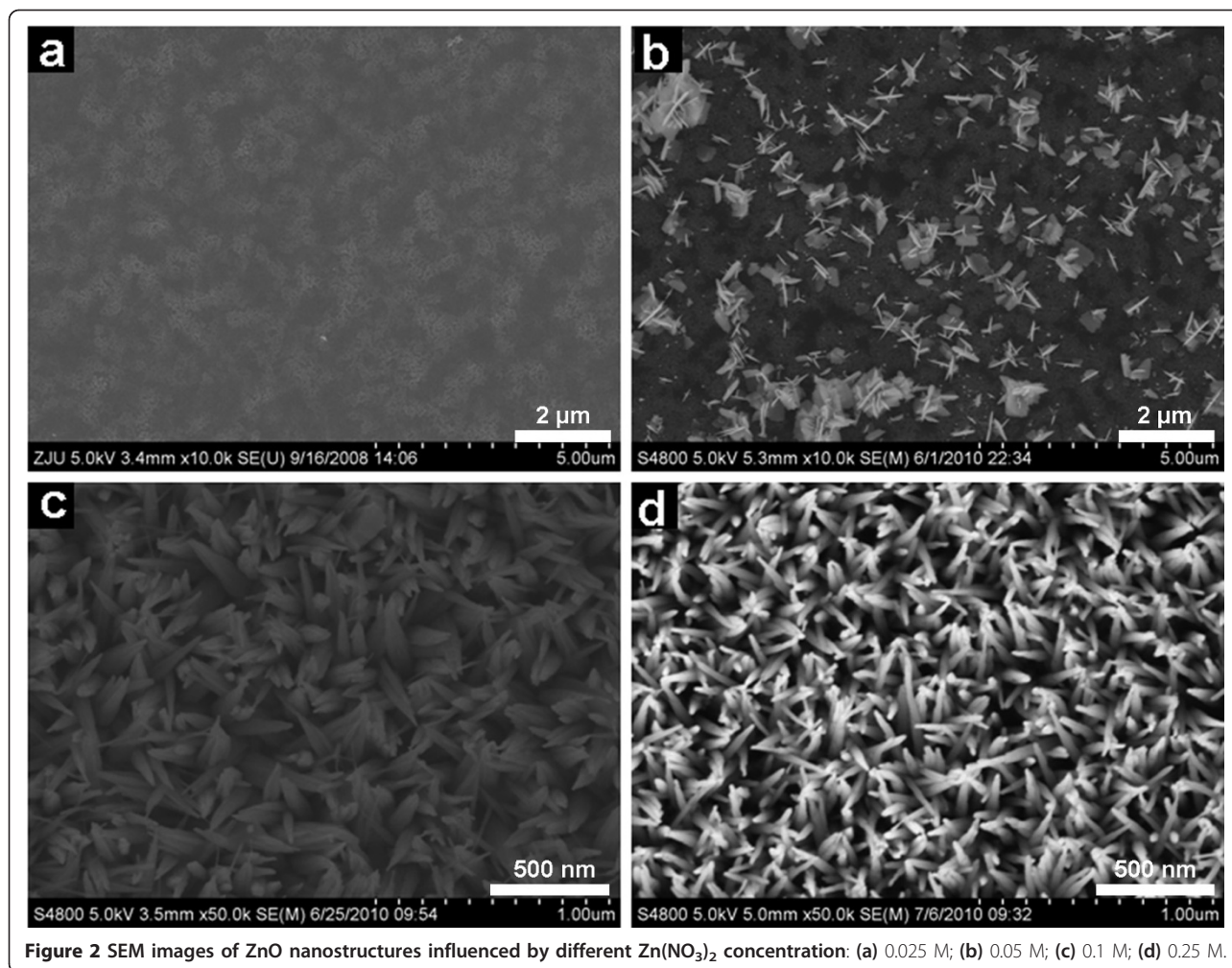


**Figure 2** SEM images of ZnO nanostructures influenced by different Zn(NO<sub>3</sub>)<sub>2</sub> concentration: (a) 0.025 M; (b) 0.05 M; (c) 0.1 M; (d) 0.25 M.

change the density or the length of nanorods, i.e., the concentrations of Zn(NO<sub>3</sub>)<sub>2</sub> or OH<sup>-</sup> ions, are rather hard to be utilized as discussed above. Since it is generally believed that high supersaturation level is favorable for nucleation, whereas low supersaturation level favors crystal growth [34], a supersaturation controlled method is developed. The degree of supersaturation (*S*) is defined as the ratio of the practical concentration (*C*) and the saturated concentration (*C<sub>s</sub>*) of Zn<sup>2+</sup> ions in the solution:

$$S = C/C_s \quad (3)$$

The original crystallization with a high ions concentration is generally a nucleation controlled process. For the following process of ZnO nanorods growth, the concentration of Zn<sup>2+</sup> ions becomes a controlling factor and the growth mediums with different *S* could influence the dimension and density of arrays.

With the same ZnO seed-layer and equivalent concentration, the different volume of growth solution strongly

influenced the density and length of the ZnO nanorods, as shown in Figure 3. When the ZnO seed-layer was dipped in the 2-mL growth medium and soaked for 2 h at room temperature (approx. 25°C), a relatively sparse, low dimension, and poorly alignment ZnO nanorods were synthesized, with an average length of 170 nm (Figure 3a). In the case of 10-mL growth medium, the higher density of ZnO nanorods compared with sample A is observed in Figure 3b1, with an average length of 365 nm. When the volume of growth solution increased to 20 mL, ZnO nanorods synthesized on substrate were densely packed and well aligned (Figure 3c1). The SEM cross-sectional image (Figure 3c2) shows the ZnO nanorods are 1100 nm in length. These results mean although the initial Zn<sup>2+</sup> ions concentrations are exactly the same, while the different absolute quantities of Zn<sup>2+</sup> ions (different supersaturation degree) do affect the growth of ZnO nanorods.

In normal conditions, the growth rate slows with time as the Zn<sup>2+</sup> ions concentration decrease and eventually equilibrium state in the solution is reached. However, the whole growth processes of ZnO nanorod arrays were in a

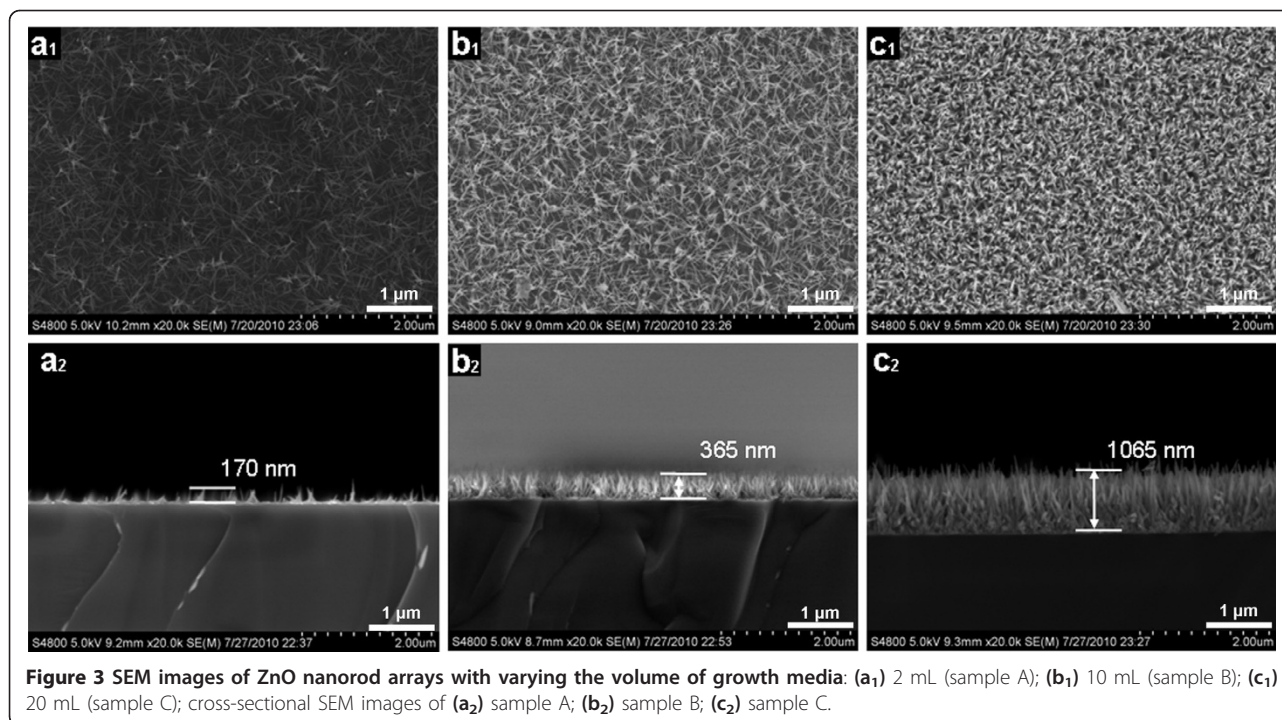


**Figure 3** SEM images of ZnO nanorod arrays with varying the volume of growth media: (a<sub>1</sub>) 2 mL (sample A); (b<sub>1</sub>) 10 mL (sample B); (c<sub>1</sub>) 20 mL (sample C); cross-sectional SEM images of (a<sub>2</sub>) sample A; (b<sub>2</sub>) sample B; (c<sub>2</sub>) sample C.

nonequilibrium state because several hours after taking out samples, there was still precipitation formed from the solution. From the results discussed above, we know that the concentration of  $\text{Zn}(\text{NO}_3)_2$  and the supersaturation degree of solution should be maintained at a certain value to guarantee the nucleation and the growth processes of ZnO. When the initial concentration is same, the nucleation rate should be equivalent in different volume media with the homolographic ZnO-coated substrates. However, the  $\text{Zn}^{2+}$  consumption of nucleation process strongly influences the absolute value of  $\text{Zn}^{2+}$  ions especially in the minimum growth volume which results in the changing of  $\text{Zn}^{2+}$  ions concentration. As the reaction processes,  $\text{Zn}^{2+}$  concentration and  $S$  decrease gradually, but the decreasing rates in different volume media are not the same. AAS results confirm that the final  $\text{Zn}^{2+}$  concentrations in 2, 10, and 20 mL medium are 0.087, 0.115, and 0.124 M, respectively. The nucleation and growth rate along the  $c$ -axis direction are limited by the concentration of the zinc ions in the medium. Therefore, in the growth medium with the smallest volume (2 mL), the nucleation and the growth of ZnO nanorods will quickly stop when the  $\text{Zn}^{2+}$  concentration decreases to the certain value. While in the growth medium with larger volume, the nucleation of ZnO can be increased and the nanorod growth can be accelerated.

#### Phase and structure of ZnO nanorods

The crystallinity of ZnO nanorod arrays grown on Si substrate with different density and length were studied

by X-ray diffraction (XRD), as shown in Figure 4. The diffraction peaks in the typical XRD patterns confirm that the ZnO crystals are hexagonal wurtzite structure ( $p6_3mc$ ). A sharp (002) diffraction peak indicates that most of the 1D ZnO nanorods grow preferentially along the [0001] direction ( $c$ -axis) and perpendicularly to the substrate. In addition, it can be seen that, with the evident enhancement of the peak intensity, the crystalline is abruptly improved, especially indicated by the sharp (002) diffraction peak.

Figure 5a shows the TEM images of sample C and it can be seen that the diameter difference of nanorod between tip and root is nearly 60 nm. In addition, the selected area electron diffraction (SAED) pattern (Figure 5b) reveals that ZnO nanorods grown at room temperature are monocrystalline. The corresponding region of high-resolution TEM (HRTEM) image (Figure 5c) exhibits the lattice spacing between the adjacent planes is 0.26 nm, which matches well with the (002) crystal planes of wurtzite ZnO. The HRTEM results further confirm that the  $c$ -axis orientation is the preferential growth direction of the single-crystalline ZnO nanorods which correspond to the XRD results.

#### Wettability and electrowetting properties of ZnO nanorod arrays

The superhydrophobic materials have risen worldwide research interest because of their considerable promise for potential applications, such as self-cleaning surfaces and lab-on-chip devices [35]. It is still a challenge to

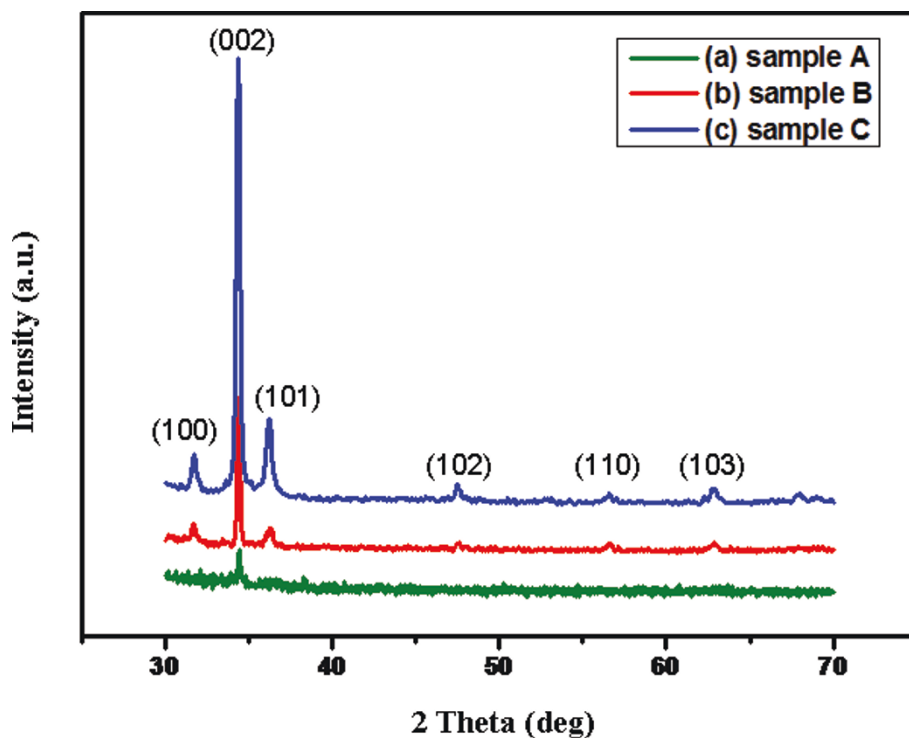


**Figure 4** XRD patterns of ZnO nanorod arrays with different volumes of the growth media: (a) 2 mL (sample A); (b) 10 mL (sample B); (c) 20 mL (sample C).

change the wettability behavior on superhydrophobic surfaces. In this study, we present a comparison of the wettability and electrowetting performances among ZnO nanorod arrays with different densities and dimensions. The wettability measurements of ZnO nanorod arrays on Si substrate with different densities and dimensions (samples A-C) and ZnO seed-layer film show that the water contact angle ( $\theta$ ) is 74.0°, 103.4°, 131.2°, and 93.5°, respectively (Figure 6a,b,c,d).

Surface wettability is believed to be regulated by both the chemical composition and the surface geometric structure. Concretely, following the rule of Zisman, wetting surfaces possess high surface energy and nonwetting surfaces are characterized by low surface energy [36]. Furthermore, the Wenzel model predicts that the contact angle of a hydrophilic surface ( $\theta < 90^\circ$ ) decreases when its surface is roughened, while roughening a nonwetting surface ( $\theta > 90^\circ$ ) always increases its hydrophobicity [37]. In this study, the surface energy could be decreased because the ZnO nanorod arrays, which grow preferentially along *c*-axis direction on the ZnO seed-layer film, and have the lowest surface free energy compared with other random orientations of ZnO films. This can promote the hydrophobicity of surfaces from the rule of Zisman. In addition, the contact angle of ZnO seed-layer film is larger than  $90^\circ$  which could be

considered to be hydrophobic. Therefore, the hydrophobic property could be increased when the surface is roughened according to Wenzel model.

In cases of samples B and C, both of the low surface energy and the high roughness enhance the hydrophobicity of surface. With the increase of density and length of ZnO nanorod arrays, the roughness of the nonwetting film surface increases evidently which results in the enhancement of hydrophobicity in samples B and C. However, the wettability of sample A is not consistent with this regulation. It is supposed that the lower crystalline degree and higher oxygen deficiency of short and sparse nanorods increase the surface energy of sample A, which exceeds the effect from surface roughness. Consequently, sample A turn to a hydrophilic surface.

The electrowetting relies on the modification of contact angle by the application of an electrical potential between the conducting substrate and the liquid droplet (Figure 7), which starts from the electrocapillarity phenomenon. For 3- $\mu$ L droplets of deionized water, the contact angle changes of samples A, B, C, and ZnO seed-layer film were observed by adjusting voltages from 0 to 60 V. Figure 8a1-d1 and 8a2-d2 shows the performance of droplets when voltages at 0 and 60 V were added. As can be observed in Figure 8, the contact angle change of sample C after applying a voltage in the



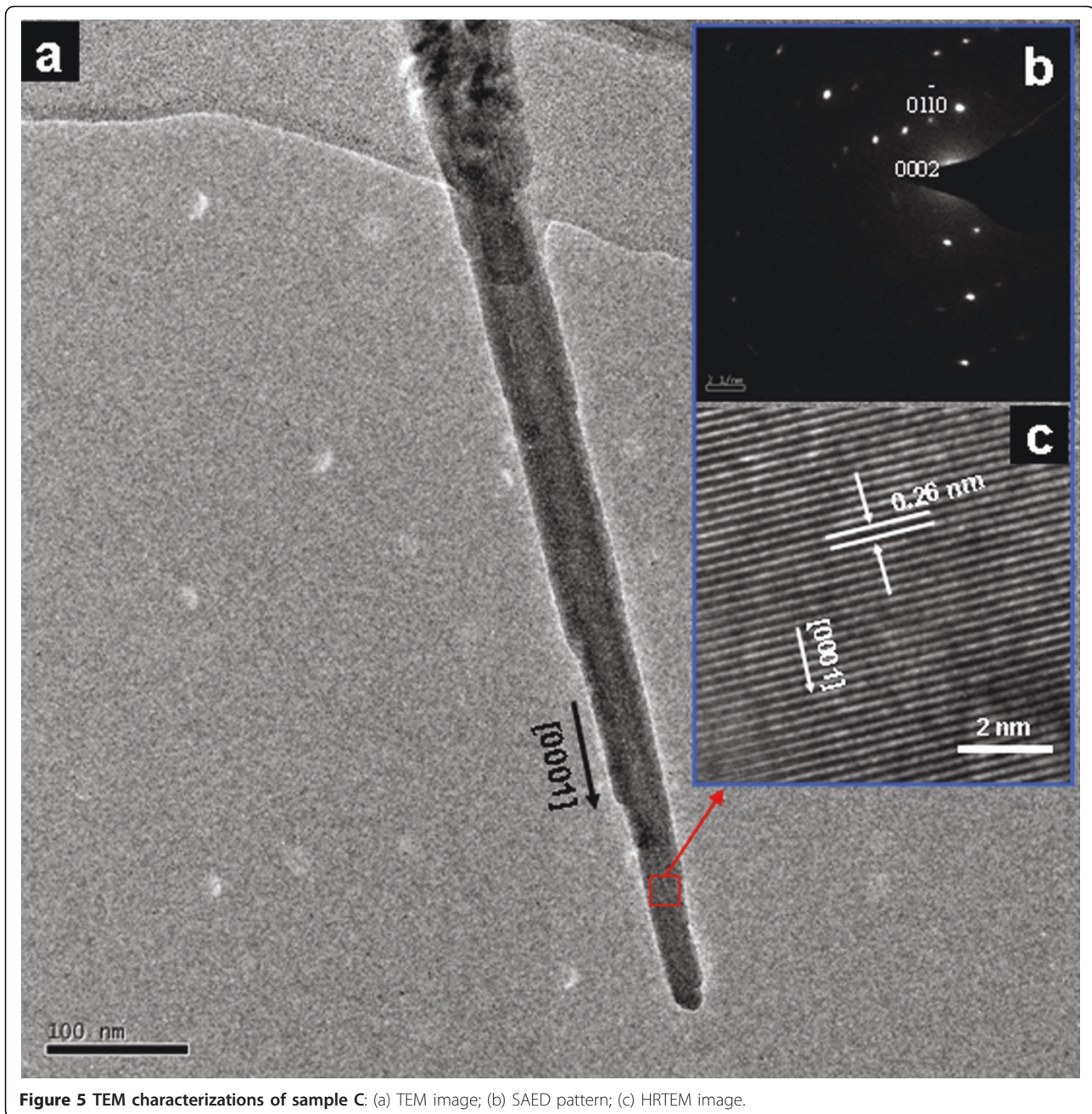


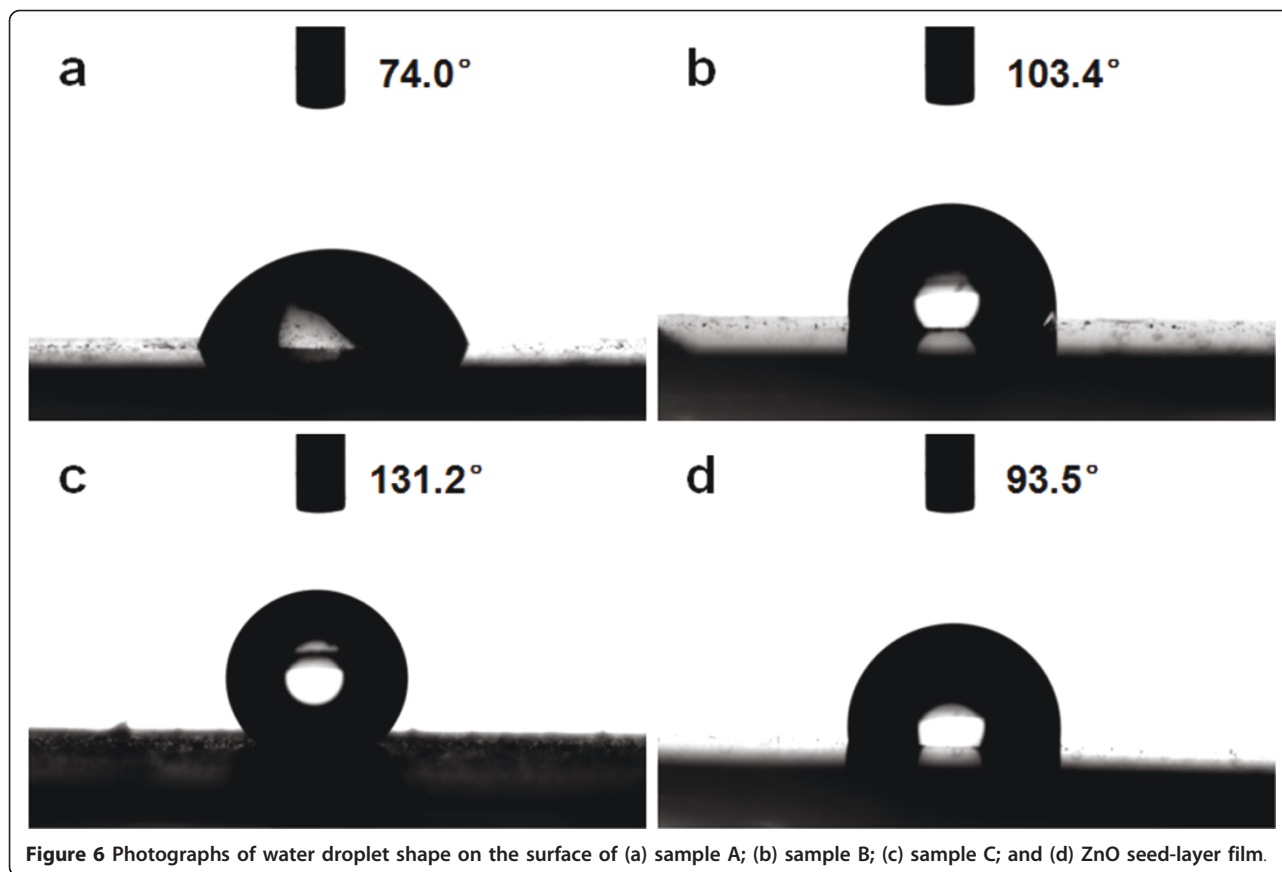
**Figure 5** TEM characterizations of sample C: (a) TEM image; (b) SAED pattern; (c) HRTEM image.

0 to 60 V range is as large as 95° and the sample A with lower density and length exhibits a poor electrowetting property which only a 29.7° change can be seen. The electric field results in a distribution of charge that alters the surface free energy, causing the droplet to spread on the surface [38]. The lower density of ZnO nanorod array, the fewer free energy changes when apply a voltage, so that the electrowetting property of ZnO film seems to be limited (Figure 8d1, d2). The gradual electrowetting responses were recorded and shown

in Figure 9. This gradual response has its advantage for applications such as electrooptics and so on [39].

#### Field emission properties of ZnO nanorod arrays

It is well known that ZnO 1D nanostructures with different shapes, such as nanowires, nanorods, and nanotubes, have been observed to have better field emission properties than the traditional materials. Commonly, the excellent field emission performance of 1D ZnO nanorod array is believed to benefit from the geometrical



configuration of sharp tips, optimized density, and large aspect ratio [4,30]. In this study, we investigated the field emission properties of ZnO nanorod arrays with sharp tips and with different density and dimension prepared on Si substrates. The measurements of field emission were carried out in a vacuum chamber at room temperature. The  $J$ - $E$  characteristic curves of samples A-C are shown in Figure 10, which gives the field emission current density ( $J$ ) of each sample on the average electric field ( $E$ ) between the anode and the cathode. The results

show that samples B and C have obvious and stable field emission properties, and no emission current was detected from sample A even the applied voltage reached nearly 2000 V. The turn-on voltage of samples B and C is about 3.0 and 2.4 V/ $\mu\text{m}$  corresponding to a current density of 1  $\mu\text{A}/\text{cm}^2$ . It is obvious that sample C has the best field emission property with the lowest turn-on electric field and with the highest current density at the same applied electric field on samples. The better field emission performance sample C can be attributed to its high

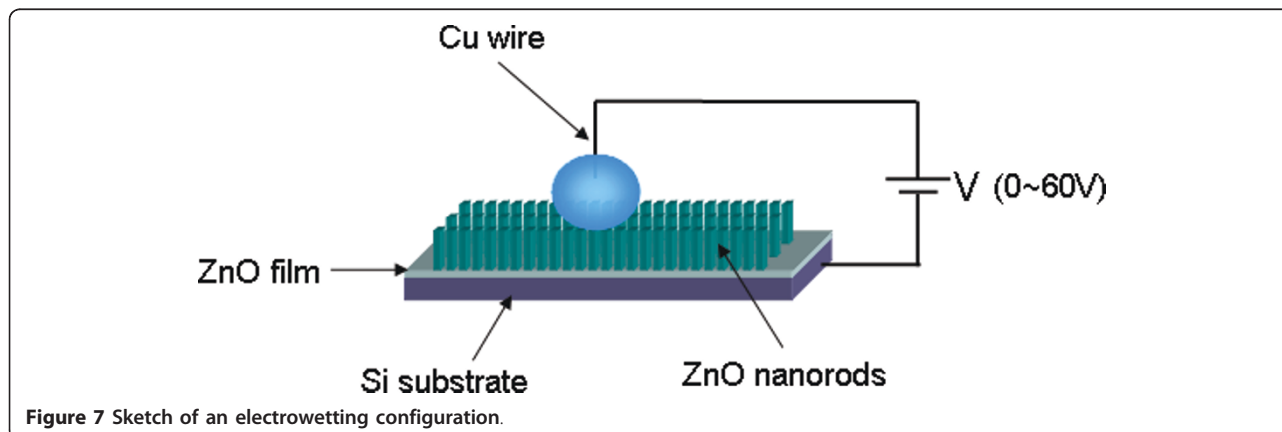
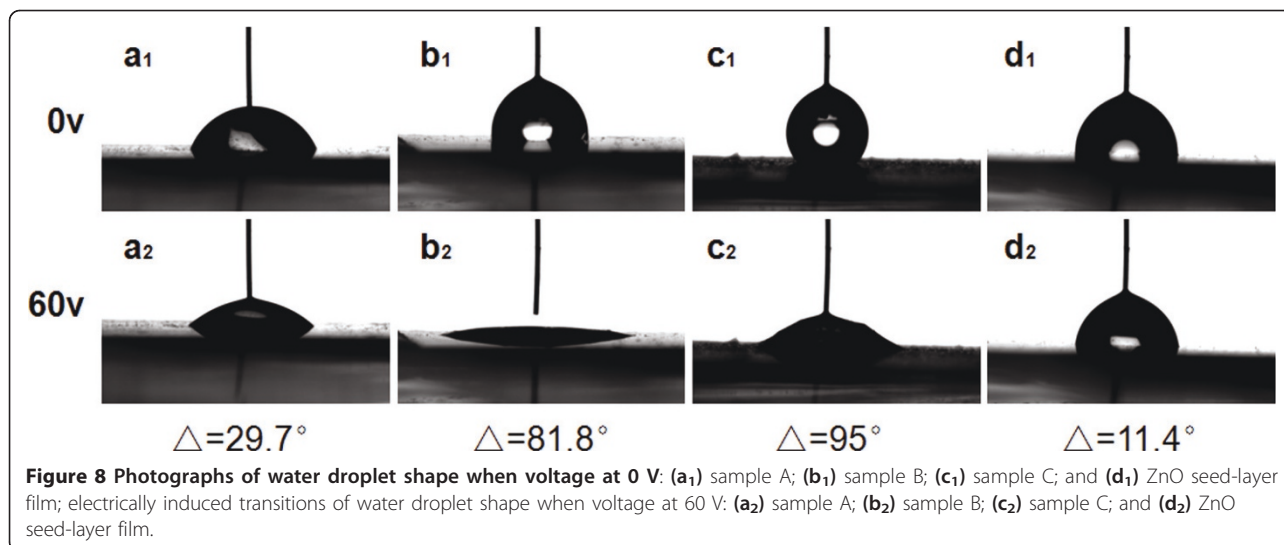


Figure 7 Sketch of an electrowetting configuration.



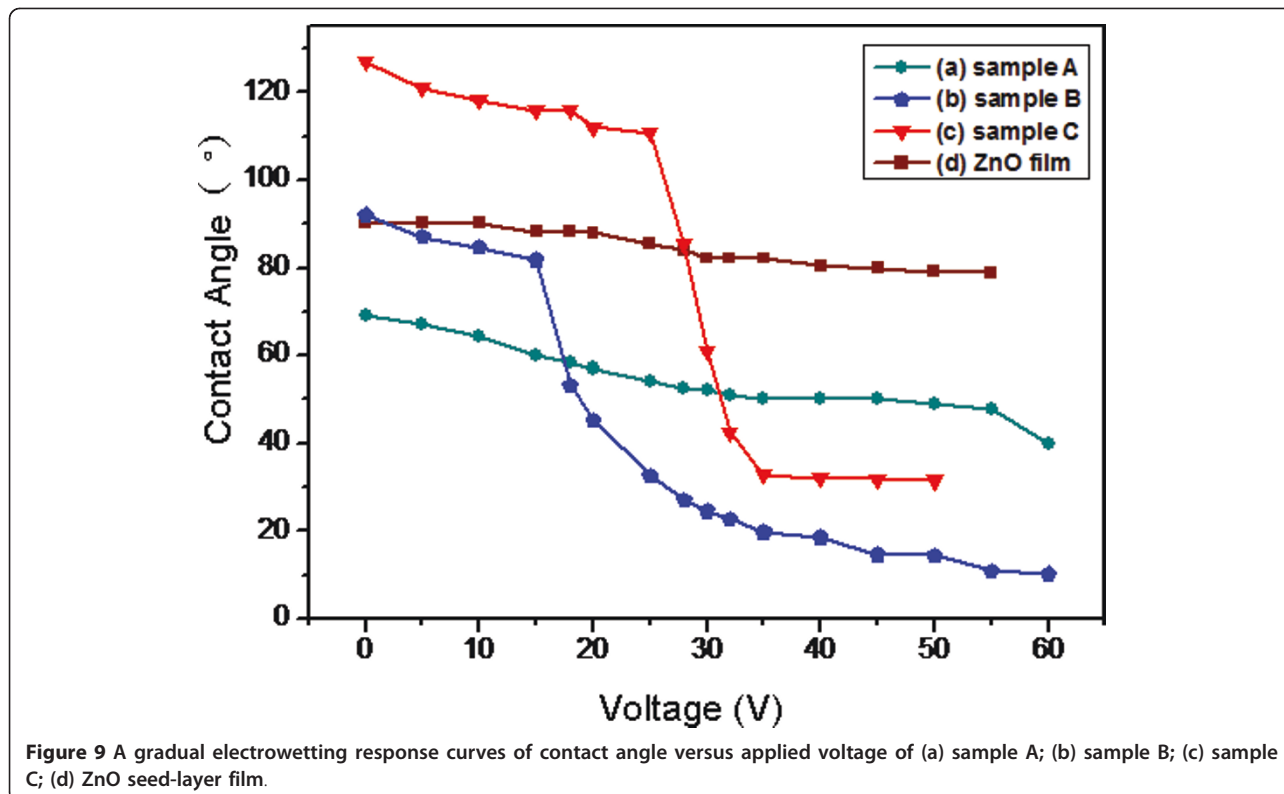


aspect ratio, which was acquired by increasing the medium volume in the present room temperature ZnO nanorods synthesis method.

### Conclusions

In summary, density and dimension controlled ZnO nanorod arrays with sharp tips were synthesized on Si substrates through a simple room temperature solution growth method (approx. 25°C) by pre-forming a ZnO

seed-layer on the substrate. Nonequilibrium growth of ZnO nanorod arrays was realized through supersaturation control in room temperature media. Concentrations of growth media, molar ratio of Zn(NO<sub>3</sub>)<sub>2</sub> to NaOH, and the supersaturation degree are the main factors in density- and length-controlled growth of ZnO nanorods. The water contact angle measurements showed that the density and dimension of nanorods would influence the surface wettability evidently. When applied a voltage in



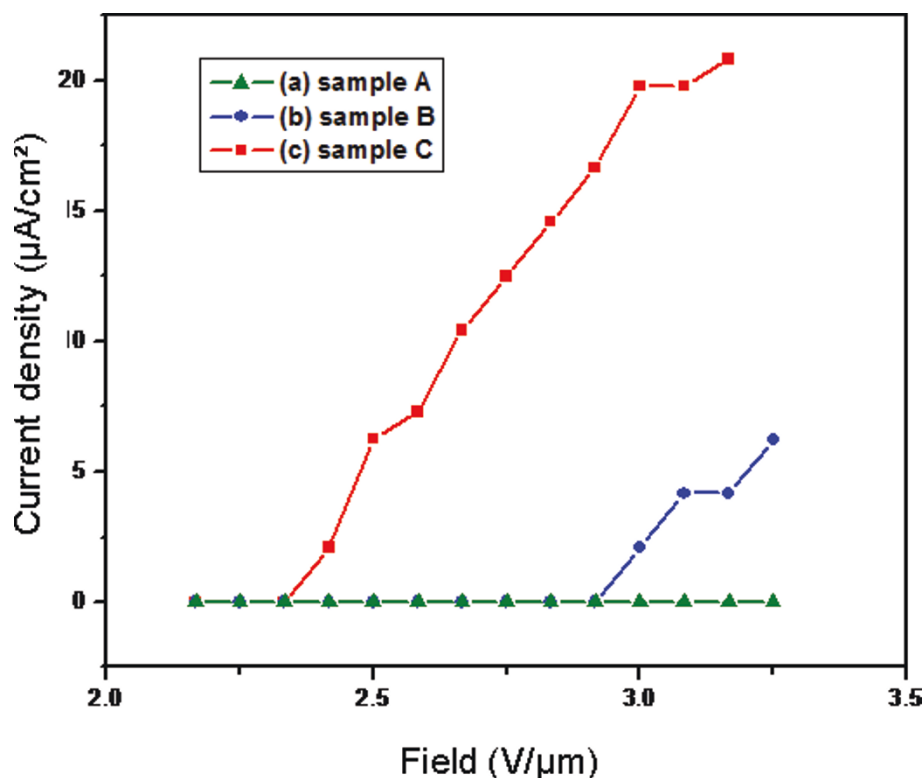


**Figure 10** Field emission properties of (a) sample A; (b) sample B; and (c) sample C.

the 0-60 V range on the droplet, the nanorod arrays performed excellent gradual electrowetting responses. The ZnO nanorod array with highest density and dimension revealed the best electrowetting property with the contact angle change of 95°. The field emission property was also optimized by changing the nanorods density and dimension. These demonstrate the present room temperature solution method is an effective way to obtain high-quality controllable ZnO nanorod arrays with potential applications for future nanodevices.

#### Abbreviations

AAS: atomic absorption spectroscopy; HRTEM: high-resolution TEM; SAED: selected area electron diffraction; TEM: transmission electron microscope; XRD: X-ray diffraction.

#### Acknowledgements

This study was financially supported by the National Nature Science Foundation of China (Grant nos. 51072178 and 81071258).

#### Authors' contributions

QL designed and carried out the experiment, statistical analysis and participated in the draft of the manuscript. KC and WW supervised the research and revised the manuscript. CS, PD, GS and GH offered the technique supports. All authors read and approved the final manuscript.

#### Competing interests

The authors declare that they have no competing interests.

Received: 7 April 2011 Accepted: 27 July 2011 Published: 27 July 2011

#### References

1. Ahn CH, Mohanta SK, Lee NE, Cho HK: Enhanced exciton-phonon interactions in photoluminescence of ZnO nanopencils. *Appl Phys Lett* 2009, **94**:261904.
2. Liang WJ, Yuhua BD, Yang PD: Magnetotransport in Co-doped ZnO nanowires. *Nano Lett* 2009, **9**:892.
3. Joshi A, Aswal DK, Gupta SK, Yakhmi JV, Gangal SA: ZnO-nanowires modified polypyrrole films as highly selective and sensitive chlorine sensors. *Appl Phys Lett* 2009, **94**:103115.
4. Xiao J, Zhang XX, Zhang GM: Field emission from zinc oxide nanotowers: the role of the top morphology. *Nanotechnology* 2008, **19**:295706.
5. Bai XD, Wang EG, Gao PX, Wang ZL: Measuring the work function at a nanobelt tip and at a nanoparticle surface. *Nano Lett* 2003, **3**:1147.
6. Yan CL, Liu J, Liu F, Wu JS, Gao K, Xue DF: Tube formation in nanoscale materials. *Nanoscale Res Lett* 2008, **3**:473.
7. Wang XD, Song JH, Summers CJ, Ryou JH, Li P, Dupuis RD, Wang ZL: Density-controlled growth of aligned ZnO nanowires sharing a common contact: a simple, low-cost, and mask-free technique for large-scale applications. *J Phys Chem B* 2006, **110**:7720.
8. Özgür Ü, Alivov Ya I, Liu C, Teke A, Reshchikov MA, Doğan S, Avrutin V, Cho S-J, Morkoc H: A comprehensive review of ZnO materials and devices. *J Appl Phys* 2005, **98**:041301.
9. Tian ZR, Voigt JA, Liu J, Mckenzie B, McDermott MJ, Rodriguez MA, Konishi H, Xu HF: Complex and oriented ZnO nanostructures. *Nat Mater* 2003, **2**:821.
10. Müller B, Riedel M, Michel R, De Paul SM, Hofer R, Heger D, Grützmacher D: Impact of nanometer-scale roughness on contact-angle hysteresis and globulin adsorption. *J Vac Sci Technol B* 2001, **19**:1715.
11. Lau KKS, Bico J, Teo KBK, Chhowalla M, Amaratunga GAJ, Milne WI, McKinley GH, Gleason KK: Superhydrophobic carbon nanotube forests. *Nano Lett* 2003, **3**:1701.
12. Yu HD, Zhang ZP, Han MY, Hao XT, Zhu FR: A general low-temperature route for large-scale fabrication of highly oriented ZnO nanorod/nanotube arrays. *J Am Chem Soc* 2005, **127**:2378.

13. Yang DS, Lao CS, Zewai AH: **4D electron diffraction reveals correlated unidirectional behavior in zinc oxide nanowires.** *Science* 2008, **321**:1660.
14. Wang XD, Summers CJ, Wang ZL: **Large-scale hexagonal-patterned growth of aligned ZnO nanorods for nano-optoelectronics and nanosensor arrays.** *Nano Lett* 2004, **4**:423.
15. Qurashi A, Tabet N, Faiz M, Yamzaki T: **Ultra-fast microwave synthesis of ZnO nanowires and their dynamic response toward hydrogen gas.** *Nanoscale Res Lett* 2009, **4**:948.
16. Galoppini E, Rochford JN, Chen HH, Saraf G, Lu YC, Hagfeldt A, Boschloo G: **Fast electron transport in metal organic vapor deposition grown dye-sensitized ZnO nanorod solar cells.** *J Phys Chem B* 2006, **110**:16159.
17. Wang ZL: **Zinc oxide nanostructures: growth, properties and applications.** *J Phys: Condens Matter* 2004, **16**:829.
18. Zainelabdin A, Zaman S, Amin G, Nur O, Willander M: **Stable white light electroluminescence from highly flexible polymer/ZnO nanorods hybrid heterojunction grown at 50°C.** *Nanoscale Res Lett* 2010, **5**:1442.
19. Ahsanulhaq Q, Kim JH, Kim JH, Hahn YB: **Seedless pattern growth of quasi-aligned ZnO nanorod arrays on cover glass substrates in solution.** *Nanoscale Res Lett* 2010, **5**:669.
20. Sun HK, Luo M, Weng WJ, Cheng K, Du PY, Shen G, Han GR: **Position and density control in hydrothermal growth of ZnO nanorod arrays through pre-formed micro/nanodots.** *Nanotechnology* 2008, **19**:395602.
21. Jung MH, Lee H: **Selective patterning of ZnO nanorods on silicon substrates using nanoimprint lithography.** *Nanoscale Res Lett* 2011, **6**:159.
22. Look DC, Reynolds DC, Litton CW, Jones RL, Eason DB, Cantwell G: **Characterization of homoepitaxial p-type ZnO grown by molecular beam epitaxy.** *Appl Phys Lett* 2002, **81**:1830.
23. Bae J, Hong J-I, Han WH, Choi YJ, Snyder RL: **Superior field emission properties of ZnO nanocones synthesized by pulsed laser deposition.** *Chem Phys Lett* 2009, **475**:260.
24. Yin ZY, Wu SX, Zhou XZ, Huang X, Zhang QC, Boey F, Zhang H: **Electrochemical deposition of ZnO nanorods on transparent reduced graphene oxide electrodes for hybrid solar cells.** *Small* 2010, **6**:307.
25. Shen GZ, Bando Y, Liu BD, Golberg D, Lee C-J: **Characterization and field-Emission properties of vertically aligned ZnO nanonails and nanopencils fabricated by a modified thermal-evaporation process.** *Adv Funct Mater* 2006, **16**:410.
26. Wu XF, Lu GW, Li C, Shi GQ: **Room-temperature fabrication of highly oriented ZnO nanoneedle arrays by anodization of zinc foil.** *Nanotechnology* 2006, **17**:4936.
27. Cho S, Jang J-W, Lee J S, Lee K-H: **Room temperature synthesis and optical properties of small diameter (5 nm) ZnO nanorod arrays.** *Nanoscale* 2010, **2**:2199.
28. Qian XM, Liu HB, Guo YB, Song YL, Li YL: **Effect of aspect ratio on field emission properties of ZnO nanorod arrays.** *Nanoscale Res Lett* 2008, **3**:303.
29. Ma T, Guo M, Zhang M, Zhang YJ, Wang XD: **Density controlled hydrothermal growth of well-aligned ZnO nanorod arrays.** *Nanotechnology* 2007, **18**:035605.
30. Pan N, Xue HZ, Yu MH, Cui XF, Wang XP, Hou JG, Huang JX, Deng SZ: **Tip morphology-dependent field emission from ZnO nanorod arrays.** *Nanotechnology* 2010, **21**:225707.
31. Zhao Q, Zhang HZ, Zhu YW, Feng SQ, Sun XC, Xu J, Yu DP: **Morphological effects on the field emission of ZnO nanorod arrays.** *Appl Phys Lett* 2005, **86**:203115.
32. Sun HK, Luo M, Weng WJ, Cheng K, Du PY, Shen G, Han GR: **Room-temperature preparation of ZnO nanosheets grown on Si substrates by a seed-layer assisted solution route.** *Nanotechnology* 2008, **19**:125603.
33. Zhao J, Jin ZG, Liu XX, Liu ZF: **Growth and morphology of ZnO nanorods prepared from Zn(NO<sub>3</sub>)<sub>2</sub>/NaOH solutions.** *J Europ Ceram Soc* 2006, **26**:3745.
34. Weintraub B, Zhou ZZ, Li YH, Deng YL: **Solution synthesis of one-dimensional ZnO nanomaterials and their applications.** *Nanoscale* 2010, **2**:1573.
35. Verplanck N, Coffinier Y, Thomly V, Boukherroub R: **Wettability switching techniques on superhydrophobic surfaces.** *Nanoscale Res Lett* 2007, **2**:577.
36. Zisman WA: **Relation of the equilibrium contact angle to liquid and solid constitution.** *Adv Chem Ser* 1964, **43**:1.
37. Papadopolou EL, Barberoglou M, Zorba V, Manousaki A, Pagkizidis A, Stratakis E, Fotakis C: **Reversible photoinduced wettability transition of hierarchical ZnO structures.** *J Phys Chem C* 2009, **113**:2891.
38. Verheijen HJJ, Prins MWJ: **Reversible electrowetting and trapping of charge: model and experiments.** *Langmuir* 1999, **15**:6616.
39. Dhindsa MS, Smith NR, Heikenfeld J: **Reversible electrowetting of vertically aligned superhydrophobic carbon nanofibers.** *Langmuir* 2006, **22**:9030.

doi:10.1186/1556-276X-6-477

**Cite this article as:** Li et al.: Room-temperature nonequilibrium growth of controllable ZnO nanorod arrays. *Nanoscale Research Letters* 2011 **6**:477.

**Submit your manuscript to a SpringerOpen<sup>®</sup> journal and benefit from:**

- Convenient online submission
- Rigorous peer review
- Immediate publication on acceptance
- Open access: articles freely available online
- High visibility within the field
- Retaining the copyright to your article

Submit your next manuscript at ► [springeropen.com](http://springeropen.com)